Characterization of manufacturing induced agglomerated porosites in thermosetting composites using ultrasonic immersion setup

William Lucas, Simon Alverede, Florence Saffar, Tony Valier-Brasier

CHARACTERIZATION OF MANUFACTURING INDUCED AGGLOMERATED POROSITIES IN THERMOSETTING COMPOSITES USING ULTRASONIC IMMERSION SETUP

W. Lucas[1,2], A. Simon[1], F. Saffar[1] and T. Valier-Brasier[2]

[1]DMAS, ONERA, Université Paris-Saclay, 92230 Châtillon, France
Email: william.lucas@onera.fr, alverede.simon@onera.fr, florence.saffar@onera.fr,
Web Page : https://www.onera.fr/fr
[2]Institut Jean Le Rond d'Alembert, Sorbonne Université, 75005 Paris, France
Email : tony.valier-brasier@sorbonne-universite.fr,
Web Page : http://www.dalembert.upmc.fr/ijlrda/

Keywords: Carbon Fiber Reinforced Polymers, Non-destructive testing, Porosity, Ultrasonic

Abstract
This study aims to highlight the limitations of the classical ultrasonic testing methods in assessing the porosity level in CFRP composites. From the manufacturing perspectives, samples of thermosetting composite materials with unidirectional fiber orientation, featuring diverse distributions and volume fractions of porosity, are prepared in autoclave. Two kind of porosity distribution are studied, the first one with residual porosities all over the sample thickness and the second one with porosities clustered in a single interface between two plies. These samples undergo testing thanks to an immersion ultrasonic scanning method, employing two planar transducers to measure the transmission through the sample. The attenuation of elastic waves is then calculated comparing the amplitude of the Fourier-transformed acquired signals. It is well known that ultrasonic attenuation can be directly link to void rate but the results of the scans reveal the incapacity of this classical method to asses clustered porosities. Hence, a complementary parameter made to emphasize the potential localized nature of the porosities is proposed.

1. Introduction

Carbon Fiber Reinforced Polymers (CFRPs) are widely used in the aerospace industry for their outstanding mechanical properties and the mass gains resulting from their low mass density [1]. During the manufacturing process, defects such as porosities due to entrapped air can be introduced in the material, affecting its mechanical properties [2], [3]. Uniformly distributed and small-sized porosities, also called residual porosities are tolerated up to a threshold limit of 2% of the volume fraction for aircraft applications [4]. However, the distribution is frequently non-uniform, leading to the formation of local clusters of porosity that induce a significantly higher risk for the mechanical integrity of the structure compared to the residual porosities [5]. Therefore, accurate characterization of porosities is crucial to avoid unnecessary rejection of expensive components and to ensure their integrity. Ultrasonic methods, which rely on velocity and attenuation measurements, are commonly employed for this purpose but are limited to samples with a uniform distribution of porosity [6], [7]. As of now, addressing agglomerated porosities still remains a scientific challenge.
In this context, the goal of this proceeding is to present a quantitative comparison between ultrasonic measurements made in composite containing residual or clustered porosities. The first step lies in manufacturing samples with partially controlled generation of initial defects. For this purpose, two techniques are used in order to reproduce the various distribution one might encounter when manufacturing CFRP composites in the industry. Then these samples are probed with an immersion ultrasonic through-transmission setup. The classical way of processing the signal to get the attenuation

due to the porosities is then presented. Finally, the experimental results of the ultrasonic testing are exhibited and discussed. In particular, a complementary parameter that can be used in order to overcome the limitation of the classical method is introduced.

2. Development of porous composite materials

2.1. Prepreg presentation and processing in the autoclave

In the present study, the considered materials are thermosetting CFRP composites from Hextow® made of the M21ev epoxy resin. The laminate is made from a stack of 16 plies unidirectional laminate. This layup is cured in an autoclave with specifically designed curing cycles depending on pressure, temperature and vacuum level. A preimpregranted sheet is 0,18 mm thick and exhibits a fiber volume fraction of 66 %. The diameter of a single fiber is around 5 µm. Two different methods are used in order to generate porosities in the plate. The first one aims to reproduce residual porosities and consists of generating randomly distributed voids of small size in the material, by modifying the pressure of the curing cycle. The second one is a two-step method allowing to locate the porosities at a specific chosen depth in the laminate.

2.1.1. Residual porosity

The first method consists of generating different ranges of porosities by modifying the pressure level of the curing cycle. Gradually reducing pressure level for each curing cycle results in an increasingly higher porosity content in the laminate. Note that the highest-pressure level used in the experiments corresponds to the one recommended by the manufacturer. All the samples obtained by this method are listed in Table 1. The surface porosity estimation is obtained by processing the microscopic images shown in Figure 1. It consists of a threshold method achieved by filtering the darker parts of the image that corresponds to the pores and dividing the occupied surface by the whole surface. As is visible in Figure 1, the entrapped pores in the sample using this curing technique are distributed across the whole material. Moreover, the samples thickness is evaluated with a caliper. It can be observed that a when the applied pressure is lower, the obtained sample is thicker.

Table 1. List of the samples of composite with residual porosity

Reference name	*Thickness (mm)*	*Pressure Level in the autoclave (bar)*	*Surface Porosity estimation (%)*
W_{UD2}	3.14 ± 0.02	2	1.45 ± 0.65
W_{UD3}	3.06 ± 0.02	4	0.45 ± 0.53
W_{UD4}	3.00 ± 0.02	6	0.19 ± 0.37

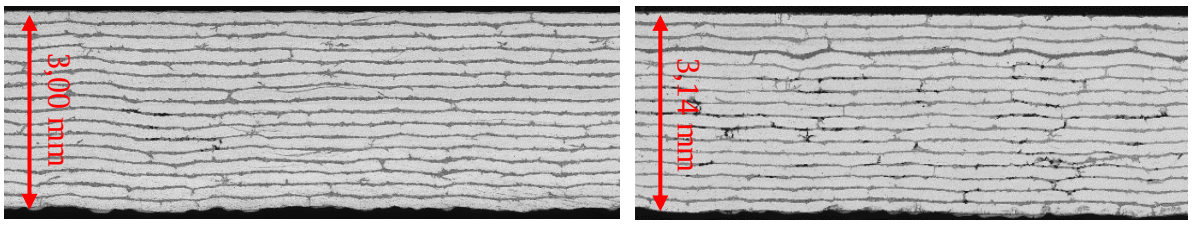

Figure 1. Optical microscope observations of the edge after micrometric size polishing of the composite samples: W_{UD4} (left) and W_{UD2} (right).

2.1.2 Clustered porosities

In order to reproduce clustered porosities i.e. locally highly concentrated porosities in a composite sample, a different approach is used. The method is based on a two-stage curing of the composite. Initially, two or three prepregs are stacked and cured in the autoclave using a modified curing cycle for

pressure and temperature, aiming to trap pores between the plies. Only vacuum (i.e. no pressure) to generate a high porosity rate and relatively low curing temperature ($\sim 150\,°C$) to only initiate the polymerization of the resin, are the first step. The porosities locate at the interface between the plies. The number of porous interfaces can be varied by adjusting the number of plies to pre-cure. The second part of the method consists of laying up the rest of the plies placing the "pre-cured" ones at the desired depth in the stack. The laminate is then cured following the reference curing cycle. The samples obtained from this method are shown in Figure 2 and listed in Table 2. It is important to keep in mind that this manufacturing method is not to be used as a conventional method. However, the porosity distribution in these samples are representative of those that can appear in the industry, at an interface between two welded thermoplastic material for example. From Figure 2 it can be observed that sample W_{AGGLO1} and W_{AGGLO2} have one and two porous interfaces, respectively, located in the middle of the sample depth. The estimated surface porosity is lower than in the previous samples W_{UD2} and W_{UD3}. A local surface estimation of porosity is then performed by looking one ply at the time i.e. selecting the porous rich resin interface between the middle of two fibrous ones. This complementary analysis reveals a highly located porosity content in W_{AGGLO1} and W_{AGGLO2}.

Table 2. List of the samples of composite with agglomerated porosity

Reference name	*Thickness (mm)*	*Number of porous interfaces*	*Surface Porosity estimation (%)*	*Local porosity estimation over 1 ply (%)*
W_{AGGLO1}	2.98 ± 0.02	1	0.13 ± 0.03	2.26
W_{AGGLO2}	2.98 ± 0.02	2	0.48 ± 0.27	2.94

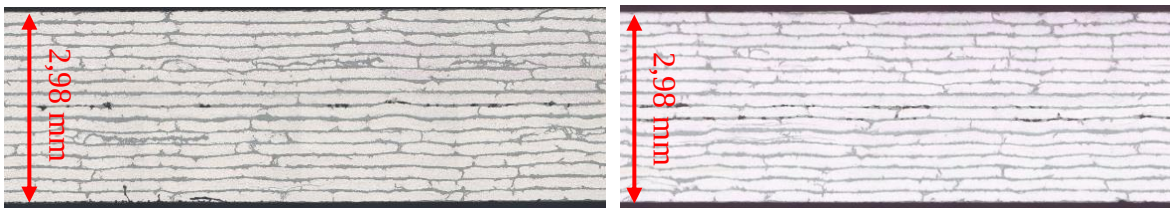

Figure 2. Optical microscope observations of the edge after micrometric size polishing of the composite samples: W_{AGGLO1} (left) and W_{AGGLO2} (right).

3. Ultrasonic characterization

3.1. Experimental setup

The experimental ultrasonic testing setup consists of an immersion through-transmission experiment. This technique allows an easy and reproductible coupling between the sensors and the samples. Two planar transducers are aligned and facing each other. Special attention must be paid to align the transducers, employing manual micro-controllers and goniometers. Between them, a sample is placed, held by a system mounted on two motorized axes allowing for the selection of the probed area by the emitter on the sample. In order to effectively distinguish the different echoes arising from reflections and transmissions through the laminate, the chosen transducers are a pair of Olympus® V309 (planar transducer) with a center frequency of 5 MHz and a diameter of 12,7 mm. The -6 dB from maximum frequency bandwidth of the transducers ranges from 2,4 to 7,5 MHz and the distance between the emitter and the sample is 20 cm. It is chosen to be larger than the far-field distance of the emitter. In this zone, ultrasonic beam is considered to be well formed and the generated waves can be modelized as plane waves. Therefore, the circular local inspected area, defined as the zone where ultrasonic energy is higher than the maximum -6 dB and calculated thanks to CIVA software, is 10 mm diameter. A schematic representation of the system is presented in Figure 3 alongside the explanation of the signal windowing in the following section.

3.2. Signal Processing

To assess the viscoelastic behavior of the composite, the wavenumber of the plate k_m is expressed as $k_m = \frac{\omega}{c_m} - i\alpha_m$ with ω the angular frequency, c_m the phase velocity and α_m the attenuation. To identify parameters α_m and c_m, the employed method consists of comparing the signal of the elastic wave measured through the sample $s_m(t)$ to the one in water $s_0(t)$ without moving the transducers. In order to consider the composite as an infinite medium, the part of the signal corresponding to the direct path through the sample is selected by numerically applying a Tuckey window as it is shown in Figure 3.

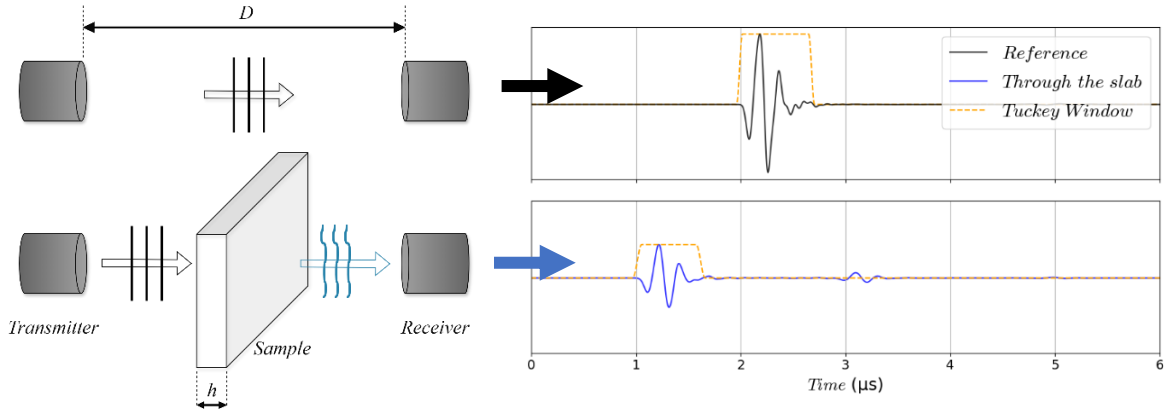

Figure 3. Schematic representation of the experiment (left). Reference signal $s_0(t)$ is in black and through the coupon $s_m(t)$ in blue (right).

Then, assuming $A(\omega)$ as an electro-mechanical coupling coefficient depending on the Fourier transform of the electric measured signals and the piezo-electrical responses of the transducers, the two spectra can be expressed as followed :

$$\begin{aligned} S_0(\omega) &= A(\omega)e^{-ik_0 D}, \\ S_m(\omega) &= A(\omega)\tau e^{-ik_m h}e^{-ik_0(D-h)}, \end{aligned} \tag{1}$$

where k_0 is the wave number in water, D is the distance between the two transducers and h is the sample thickness. τ is the transmission coefficient obtained from the mass density ρ_m and ρ_0 (respectively for the slab and the water) and the propagating vectors k_0, defined as [8] :

$$\tau = t_{0\to m} \cdot t_{m\to 0} = \frac{4\rho_0 k_0 \rho_m k_m}{(\rho_0 k_m + \rho_m k_0)^2}. \tag{2}$$

Expressing the ratio of the spectrums from equation (1) allows one to get rid of $A(\omega)$:

$$\frac{S_m(\omega)}{S_0(\omega)} = \tau \frac{e^{-ik_m h}e^{-ik_0(D-h)}}{e^{-ik_0 D}} = \tau e^{-i(k_m - k_0)h}. \tag{3}$$

This leads to the analytical formulas for the velocity and attenuation of elastic waves through the laminate :

$$c_m = \frac{\omega h}{\arg(\tau) + k_0 h - \arg\left(\frac{S_m}{S_0}\right)} \quad ; \quad \alpha_m = -\frac{1}{h}\left[\ln\left|\frac{S_m}{S_0}\right| - \ln(\tau)\right]. \tag{4}$$

These two parameters are calculated through an iterative process over the initially unknown transmission coefficient τ, which depends on the unknown k_m parameter. By injecting the calculated values for c_m and α_m at each step, the process quickly converges to a stable value of the coefficient.

4. Results

4.1 Classical ultrasonic porosity assessment

The ultrasonic measurements are performed using the experimental protocol explained in section 3. The results are displayed as a comparison between the two types of samples (residual or agglomerated porosities) in order to investigate the differences emerging from the ultrasonic testing. As an example, Figure 4 displays signals acquired at the center of samples.

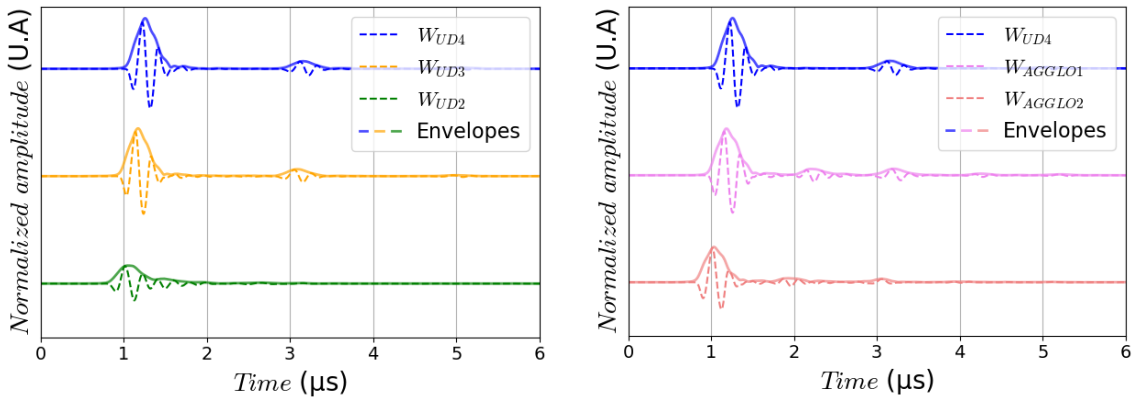

Figure 4. Signals acquired through the samples: (left) with residual porosities; (right) with agglomerated porosities. Signal through W_{UD4} is shown as a reference.

The signal through sample W_{UD4} corresponds to the signal emerging from a presumed "free-flaws" area, selected as the less attenuated signal i.e. the one with the highest first echo amplitude (called after the ballistic echo). This ballistic part is followed by a second echo corresponding to a round trip in the sample, called the backwall echo. There is almost no energy in the part between the echoes when the composite sample is almost non-porous like W_{UD4}. In W_{UD3} a slight reduction of the ballistic echo is observable resulting from the energy losses due to the multiple interactions of the wave with the pores. W_{UD2} exhibits the same behavior but with even more losses. Moreover, the shape of the ballistic signal is affected by the pores and the backwall echo is almost non-observable. On the right part of Figure 4, a reduction of the ballistic echo is observed but there is an additional echo between the ballistic and the backwall echo. It is explained by the localized nature of the porosity in these samples. By processing these signals with the method described in the previous section, the ultrasonic attenuation is assessed and presented in Figure 5. Results on the left side show an increase in attenuation with frequency and with the amount of porosity. The higher the porosity content, the higher the resulting attenuation which is an already well-established observation in the literature [6]. It goes the same way for the samples with localized porosities. Nonetheless, the overall porosity concentration is lower for W_{AGGLO1} and W_{AGGLO2} which leads to a lower attenuation. The curves can then be fitted by a quadratic model inspired by Kelvin-Voigt model [8] :

$$\alpha(f) = A \cdot \left(\frac{f}{f_0}\right)^2. \quad (5)$$

The driving coefficient A gives information for the attenuation depending on the entire frequency range f illuminated by the transducer of central frequency f_0. Note that this model only stands for the purpose of having a frequency independent parameter for the attenuation and might not be suited for the most porous samples. It is important to be cautious when interpreting the results at the limits of the transducer's bandwidth, as the emitted energy may be insufficient for reliable measurement. Before further observations of the attenuation, it is important to note that by selecting only the ballistic signal, some information are missing. Indeed, the observed ultrasonic manifestation between the ballistic signal and the back-echo (Fig. 4) in samples W_{AGGLO} and W_{AGGLO2} are not considered by this method. Moreover, curves for W_{AGGLO1}, W_{AGGLO2} and W_{UD3} look similar eventhough their porosity content are different.

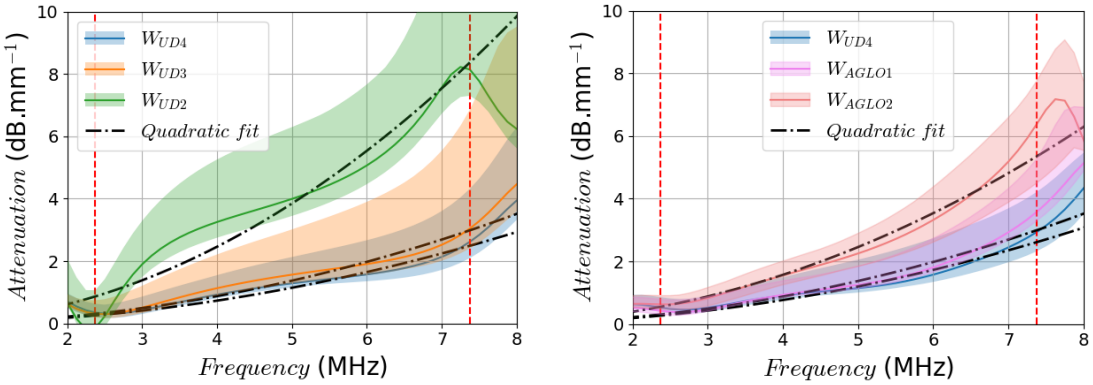

Figure 5. Measured attenuation in the samples containing residual porosities (left) and agglomerated porosities (right). The solid lines represent the attenuation at a selected point in the sample. The shaded area surrounding the curves represent the range of measured values in the samples. In red, the -6 dB bandwidth limits of the transducers.

4.2 Ultrasonic attenuation mapping

To have a better idea of the limitation of this classical method, scans are performed in the samples with a step of 1 mm between two acquired signals. The driving coefficient (Eq. 5) calculated at each point is then compared with the one obtained in the "free-flaws" area (obtained with the lowest accessible attenuation in sample W_{UD4}). Their relative variation is called R_v. The results for the residual porosities are shown in Figure 6. From this figure, one can observe that the increase of porosity leads to higher values of R_v which is logical according to the previous observations of Figure 5. The map of R_v in W_{UD4} reminds that there is always a minimum porosity level even when the sample is elaborated in the optimized conditions. This type of scanning method can also be used to identify a slightly higher-porosity region, such as the one on top of sample W_{UD3}, allowing for the selection of a part of the material without initial flaws. Finally, a threshold level for the value of R_v (determined subsequent to mechanical testing) can be fixed beyond which the porosity is considered too significant for the industrial applications. In this case, W_{UD2} could be set aside.

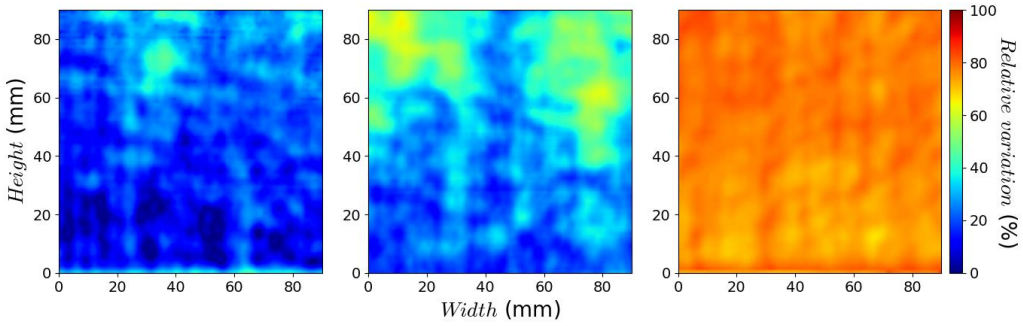

Figure 6. Map of the coefficient R_v. From left to right: W_{UD4} – W_{UD3} and W_{UD2}.

The domain of validity for these observations is limited to the residual porosity. The incapacity of this method to report on agglomerated porosity is pointed out in Figure 7. Here this type of mapping exhibits a small variation of R_v for W_{AGGLO1} that could lead to a misjudgment of the potential mechanical harm induced by the localized character of the porosity in a single interface. Using the classical attenuation method could lead to consider the sample as valid in terms of porosity concentration. For W_{AGGLO2}, the application of a threshold limit may be sufficient to state if the sample is available for industrial applications. Nevertheless, it would be advisable to conduct further inquiry into supplementary datas to validate this assertion. Finally, with this method, the results from Figure 6 and Figure 7 for W_{UD3} and W_{AGGLO1} seem similar while it is known that the porosity content is very different.

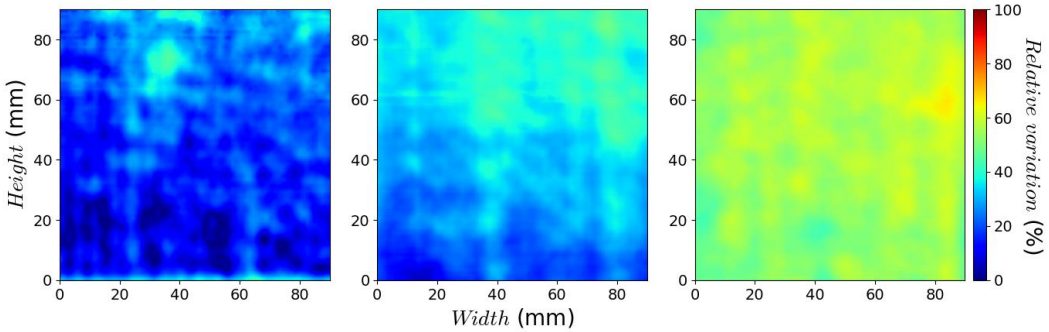

Figure 7. Map of coefficient R_v. From left to right: W_{UD4} – W_{AGGLO1} and W_{AGGLO2}.

4.3 Localized porosity investigation

Hence, a first step to investigate the localized aspect of the porosities is to analyze the part of the ultrasonic signal between the ballistic and the backwall echo. Comparing the maximum of the envelope, obtained with the Hilbert Transform of the signal in that region A_{loc} (see Figure 4), to the one of the ballistic echoes $A_{ballistic}$ can give a first parameter to analyze if there is an ultrasonic phenomenon resulting from a localized aspect of the porosity. This parameter $\boldsymbol{C_{loc}}$ is defined as:

$$C_{loc} = \left(1 - \frac{(A_{ballistic} - A_{loc})}{A_{ballistic}}\right). \quad (7)$$

The map of $\boldsymbol{C_{loc}}$ can then be computed by selecting the part of the temporal signal corresponding to the interaction of the elastic wave with the desired number of plies in the sample. Figure 8 shows the map of $\boldsymbol{C_{loc}}$ obtained by selecting a window of 4 plies in the middle of the sample depth. For the reference sample W_{UD4}, the mean value of $\boldsymbol{C_{loc}}$ is 2 % and corresponds to structural noise due to the mutilple waves reflections inside the laminates and scattering by the fibers. Therfore, a value of this parameters higher than 2 % state if there is a phenomenon going on induced by localized porosities. It is worth noting that sample W_{UD2} is not considered here as it is easily discriminated from other samples because of its much higher global ultrasonic attenuation.

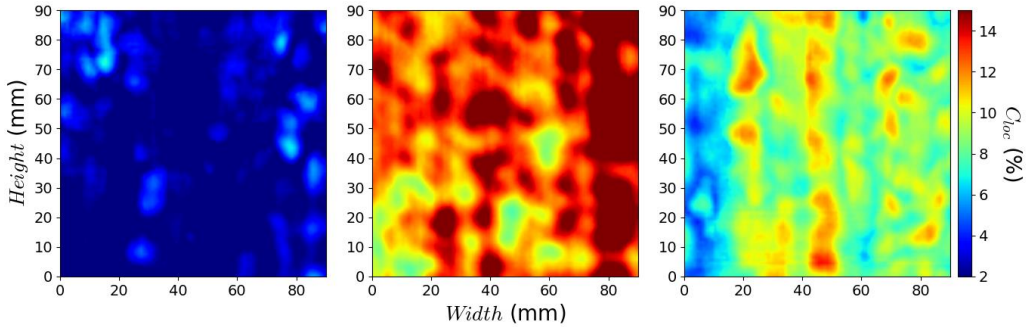

Figure 8. Map of the localization parameter $\boldsymbol{C_{loc}}$. From left to right: W_{UD3} – W_{AGGLO1} and W_{AGGLO2}.

In sample W_{UD3}, some regions present a slight increase of $\boldsymbol{C_{loc}}$ but the mean value remains at 2%. For W_{AGGLO1} and W_{AGGLO2}, $\boldsymbol{C_{loc}}$ exceeds structural noise level of W_{UD4} across all points of measurements, the mean value being respectively 13 % and 8 %. This indicates the highly located character of the porosities in the selected plies. The values differ between these two samples because of the variation in the number of porous interfaces. A higher number of porous interfaces typically result in a larger echo with a lower amplitude due to increased interactions with the pores. Conversely, when a single interface forms, it tends to produce a tighter echo with a larger amplitude. Specifically, in this case, the porous layer of W_{AGGLO1} is positioned in the middle of the sample's depth, fostering constructive interactions within the sample between the waves reflected by the borders and the porous interface. Therefore, this parameter serves as a valuable supplementary information to the classical attenuation method based on

the ballistic echo. It shows promising potential for further development. For example, it would be of interest to use a sliding window to analyse any eventual additional echo instead of a fixed one as it may give an information on the number of porous interfaces.

Conclusions

In the present paper, manufacturing methods for creating controlled porosity content in CFRP materials are presented. On one hand, a set of samples with residual porosity content are prepared, while on the other hand, an effort is made to locate the porosities at one or two interfaces between the plies of composite using a two-step curing method. Following that, a brief reminder of the classical attenuation method to asses porosity in CFRP materials is presented. The use of this method and its limitations are pointed out. In particular, it is observed that the method is not capable of detecting localized porosity. An additional parameter $\boldsymbol{C_{loc}}$ is then proposed to overcome this limitation, consisting of analyzing the amplitude of the signal envelope in the area between the ballistic echo and the back echo.
Multiple aspects of improvement can be considered to push the experiment further. From the manufacturing techniques presented, it could be possible to create a sample with controlled porosities not only in depth but also within the width and length of the samples and then to apply the technics developed in the present document. Complementary information to assess the potential mechanical harm of the localized nature of porosity should be obtained by mechanical testing. Finally, it would be interesting to collect more information on the pores by X-Ray techniques as it would give a three-dimensional estimation of the repartition of the pores, which is preferable than the surface-based estimation. Further developments to characterize the agglomerated areas still need to be investigated for a better resilience of the ultrasonic testing. It may be possible through additional numerical processing to estimate the volume fraction of the pores in a located area, utilizing an interferometric model inspired by the literature [9].

References

[1] D. Rajak, D. Pagar, P. Menezes, and E. Linul, ‘Fiber-Reinforced Polymer Composites: Manufacturing, Properties, and Applications’, *Polymers*, vol. 11, no. 10, p. 1667, Oct. 2019, doi: 10.3390/polym11101667.
[2] C. Dong, ‘Effects of Process-Induced Voids on the Properties of Fibre Reinforced Composites’, *J. Mater. Sci. Technol.*, vol. 32, no. 7, pp. 597–604, Jul. 2016, doi: 10.1016/j.jmst.2016.04.011.
[3] H. Zhu, D. Li, D. Zhang, B. Wu, and Y. Chen, ‘Influence of voids on interlaminar shear strength of carbon/epoxy fabric laminates’, *Trans. Nonferrous Met. Soc. China*, vol. 19, pp. s470–s475, Sep. 2009, doi: 10.1016/S1003-6326(10)60091-X.
[4] D. Ashouri Vajari, C. González, J. Llorca, and B. N. Legarth, ‘A numerical study of the influence of microvoids in the transverse mechanical response of unidirectional composites’, *Compos. Sci. Technol.*, vol. 97, pp. 46–54, Jun. 2014, doi: 10.1016/j.compscitech.2014.04.004.
[5] H. Liu, H. Cui, W. Wen, X. Su, H. Kang, and C. Engler-Pinto, ‘The effect of voids on the quasi-static tensile properties of carbon fiber/polymer-laminated composites’, *J. Compos. Mater.*, vol. 52, no. 15, pp. 1997–2015, Jun. 2018, doi: 10.1177/0021998317737827.
[6] Y. Ishii, S. Biwa, and A. Kuraishi, ‘Influence of porosity on ultrasonic wave velocity, attenuation and interlaminar interface echoes in composite laminates: Finite element simulations and measurements’, *Compos. Struct.*, vol. 152, pp. 645–653, Sep. 2016, doi: 10.1016/j.compstruct.2016.05.054.
[7] D. Chen, Y. Zhou, W. Wang, Y. Zhang, and Y. Deng, ‘Ultrasonic signal classification and porosity testing for CFRP materials via artificial neural network’, *Mater. Today Commun.*, vol. 30, p. 103021, Mar. 2022, doi: 10.1016/j.mtcomm.2021.103021.
[8] D. Royer and T. Valier-Brasier, *Ondes élastiques dans les solides*. in Collecion Ondes. London: ISTE éditions, 2021.
[9] A. Simon, G. Lefebvre, T. Valier-Brasier, and R. Wunenburger, ‘Viscoelastic shear modulus measurement of thin materials by interferometry at ultrasonic frequencies’, *J. Acoust. Soc. Am.*, vol. 146, no. 5, pp. 3131–3140, Nov. 2019, doi: 10.1121/1.5131026.